International Journal of Advanced Engineering Research and Science (IJAERS)
Peer-Reviewed Journal
ISSN: 2349-6495(P) | 2456-1908(O)
Vol-8, Issue-5; May, 2021
Journal Home Page Available: https://ijaers.com/
Article DOI: https://dx.doi.org/10.22161/ijaers.85.39

Looper angle and looper tension control between roll stands in hot strip finishing mills in adaptive, predictive Proportional Integral (PI) and Inverse Linear Quadratic (ILQ) control modes, with activation by means of servo valves and hydraulic cylinders

Américo Ferreira Neto, Sergio Luiz Pereira, Eduardo Mario Dias, Maria L. R. D. Scoton

GAESI – Automation and Industrial System Group – http://www.gaesi.eng.br – USP– Universidade de São Paulo – Brazil

Received: 05 Feb 2021;
Received in revised form:
16 Apr 2021;
Accepted: 11 May 2021;
Available online: 28 May 2021

***Keywords*— Hot strip finishing mills, Looper angle and tension system, Adaptive and predictive control.**

***Abstract*—** *In this article, the development of parameterization of the controller for looper control angle and tension in hot strip finishing mills is traced based on Inverse Linear Quadratic (ILQ) and Proportional Integral (PI) mode control, mainly considering, in the rolled material, thickness and width in the steel strip. Firstly, the ILQ mode approach is applied in the looper angle and looper tension, both calculated and compared with real conditions, to compensate disturbances and unmodeled dynamics in the looper, increasing or decreasing the angle position, through of Automatic Pressure Control (APC) as well as the speed reference in the previous stand rolling. Secondly, the Proportional Integral (PI) mode approach is applied in the looper angle e looper tension, where only looper angle is calculated and compared with the real condition and looper tension is calculated and applied in the open loop with use torque reference, to compensate disturbances and unmodeled dynamics in the looper. So, one set of ideal control parameters has been defined for the looper tension and looper angle, improving the performance of the overall system, always depending on the processed material, and thickness and width in the steel strip in the finishing mill. Simulation results show the effectiveness of the proposed controller compared with other methods that use only one control model for all steels' types.*

I. INTRODUCTION

Hot milling is one of the main processes in steel mills in terms of quality, cost, and energy consumption to transform steel plates into hot strip coils. This process consists of eight main steps:

a- Storage of plates proceeding from the continuous casting process in the steel mill;

b- Plate reheating furnace, using natural gas, to achieve 1240ºC;

c- Roughing mill, transforming steel plates with a thickness between 210-250 mm in steel roughing with a thickness between 20-40 mm and width between 750-2050 mm;

d- Swing shears, moving cut of roughcasts to prepare the top and tail;

e- Finishing mill, responsible for final product dimensions;

f- Cooling table to obtain mechanical properties;

This work is supported by publication, the hot strip mill looper system in IEEE Transactions on Industry Applications e Looper-Tension almost disturbance decoupling control for hot strip finishing mill based on feedback linearization in IEEE Transactions on industrial electronics.

g- Winders to roll the material in hot strip coils.

h- Storage and cooling yard for the final hot coil product obtained.

During the continuous casting process, the thickness of the plates obtained is between 210-250 mm, and the plates are reheated to achieve an extraction temperature of 1240°C; then, the thickness is reduced by means of several passes in reversible mills and the width is reduced or stretched by the edge cylinders. At the end of the thinning process, the strip thickness is typically 20 to 40 mm and the strip width is between 750 to 2050 mm, with final temperature for processing at the finishing mill stage of approximately 1050°C. After the thinning process, the strips go through the swing shears cutting process as preparation before entering the six roll stands of the finishing mill. The purpose of the finishing mill is the additional thickness reduction, with production up to 1.2 to 25 mm, which are then cooled in the outfeed table down to temperatures of approximately 870ºC, and finally rolled in the winders with a temperature of approximately 600ºC. The hot coil, final product obtained in the process, can also be processed on acold strip mill to obtain cold coils as the final product.In the finishing mill, an essential stage of the hot milling process, each roll stand is activated by an alternating current motor with speed controlled by an ASR (Automatic Speed Regulator). During the process of the finishing mill, process stability between roll stands is essential to ensure the dimensions, surface quality, and equipment availability. To allow this to happen, there are control systems between each pair of roll stands, as shown in Figure 1, in order to maintain upward pressure on the strip and ensure correct mass flow during the operation.

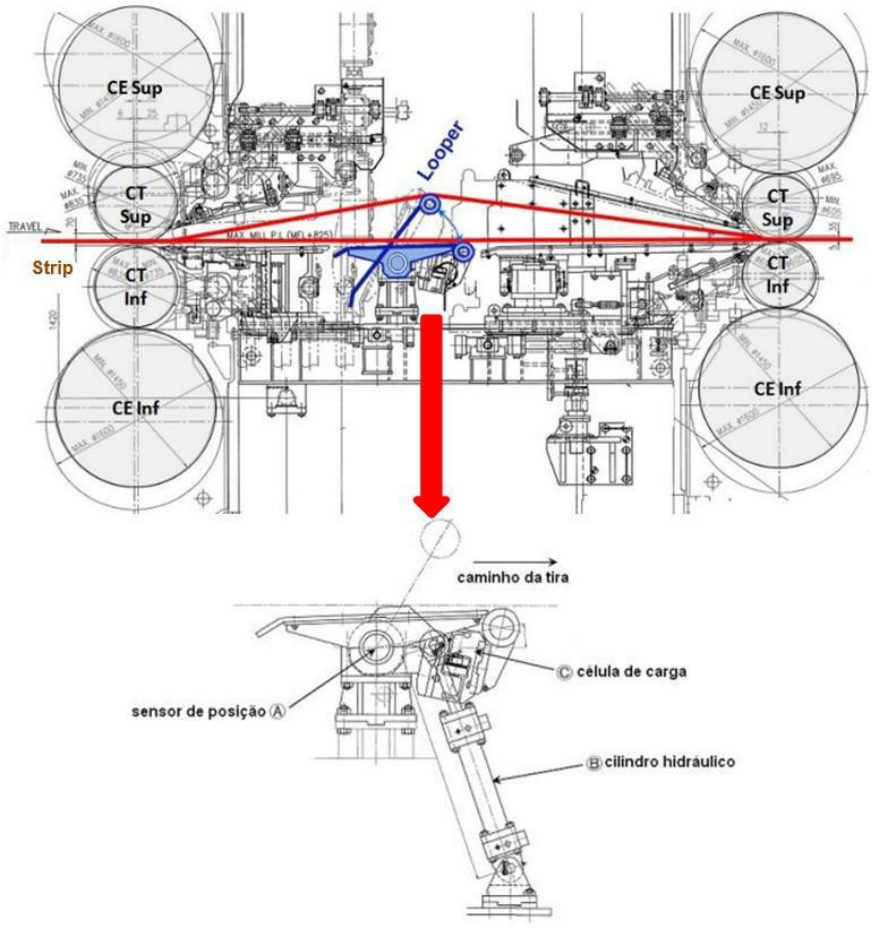

Fig.1: "Looper" and geometry between roll stands

This piece of equipment is the looper, and its movement causes strip length variations between roll stands to control mass flow imbalance and fluctuations, which are caused by four main reasons:

a- Changes in the force imposed on the roll stands by means of the Automatic Gauge Control (ACG) system or automatic thickness control;

b- Temperature heterogeneity along the strip length, from the finishing mill process or previous processes;

c- Slippage caused by the difference in speed between the strip being milled and the work cylinders in the finishing mill;

d- Changes in thickness and hardness along the strip caused by irregularities in the continuous casting process or chemical composition of the steel.

For example, in case of low strip tension between the finishing mill roll stands, the looper angle must be increased in order to increase the strip tension, as shown in Figure 2; in the opposite direction, in case of high tension between the finishing mill roll stands, the looper angle must be reduced, as shown in Figure 3, to reduce the strip tension [1]. Due to the changes in looper angle and torque, caused by changes in strip height and length between roll stands, the looper angle value must remain constant, creating a flexible system to absorb mass flow anomalies.

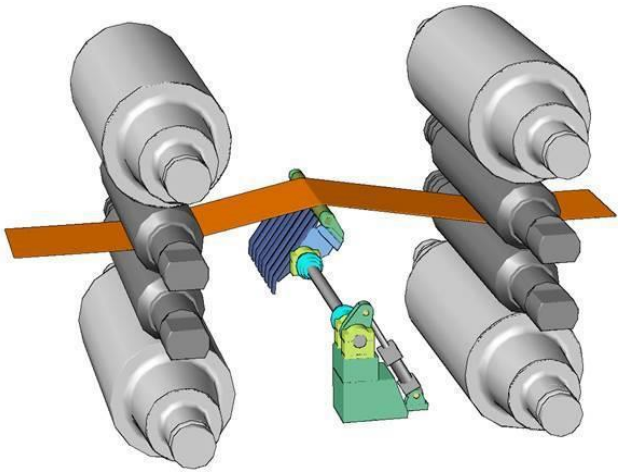

Fig.2: Increased looper angle due to low strip tension

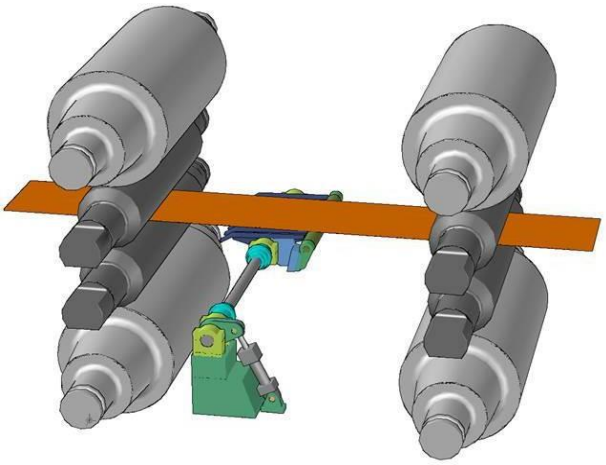

Fig.3: Reduced looper angle due to high strip tension

Perfect looper angle and torque control are critical factors to ensure strip quality and successful finishing mill operations. Due to factors such as parameter uncertainty and system disturbances of non-linear nature, looper angle and torque control are challenging projects. Some control modes are commonly used for such purposes:

a- "Inverse Linear Quadratic" (ILQ) control mode, which uses the looper angle as the main variable;

b- "Proportional Integral" (PI) control mode, conventional and not interactive, which uses the looper torque as the main variable [1];

c- Robust and adaptive control mode [2];

d- Excellent and multi-variable control [3];

e- H-infinity control mode [4].

All modes are similar to linear models regarding the references received from the output system [5, 6, 7]. Due to the non-linear nature of the system and disturbances, the controllers execute a limited range of operation. To overcome this problem, some non-linear control techniques have been proposed [8, 9, 10, 11], in these articles, the use of non-linear control techniques is effective in a wider range of work situations, for example, full non-linear controller based on a non-linear recursive method [9]; Constants were defined to account for output feedback when there is not strip tension measurement available; this system works to reject the disturbance with adaptive feedback controllers, and the simulation and online results showed the effectiveness of the controller. However, since many finishing mills have advanced equipment to collect process variables, such as strip tension meters using load cells and pressure transmitters, the availability of torque measurements

provided feedback that could make the controller more efficient.

Innovative controllers, based on "Sliding Mode Control" (SMC) [8], improve the performance of standard "Proportional Integral" (PI) controllers in the presence of friction phenomena. Since the strength must be known and becomes a simple characteristic of non-linear control systems, simulation results showed it achieved better compensation dueto disturbances caused by friction and unmodelled dynamics. The authors replaced the conventional "Proportional Integral" (PI) controller regarding looper angle by the "Sliding Mode Control" (SMC) system, while the strip tension circuit still uses the "Proportional Integral" (PI) controller. In this case, there is a shortage in the system of transitory performance and the strip speedcauses disturbances that cannot be rejected effectively.

This article applies an adaptive feedback controller in the strip tension circuit, considering the product dimensional characteristics and types of steel being milled, combining the benefits of both techniques, looper angle and torque control, using finishing mill data, acting in a predictive fashion, and improving the system global performance. As a response to the control system, using the "ILQ" and "PI" control modes, which consider looper angle and torque as the main variables, changes in position by means of a hydraulic circuit using servo valves and hydraulic cylinders. Up to the implementation of the present study in USIMINAS Hot Strip Mill N°2 in Cubatão, the finishing mill used two control modes:

a- "Inverse Linear Quadratic" (ILQ) control mode, which uses the looper angle as the main variable;

b- "Proportional Integral" (PI) control mode, conventional and not interactive, which uses the looper torque as the main variable [1];

The relation between these modes was random and completely based on operator experience, causing disadvantages in the process:

a- Occurrence of strip scrapping in the finishing mill process due to the incompatibility of the "setup" defined by the equipment operator;

b- Constant interruptions due to scrapping, significantly reducing equipment availability;

c- Product rework and deviations due to non-compliance with dimensional requirements;

d- Increased processing costs;

e- Hot strip OTIF reduction;

II. MAIN MILLED STRIP QUALITY DEFECTS AND IMPACTS ON PRODUCTION CAUSED BY INCORRECT LOOPER OPERATION

Incorrect looper operation during the mass flow imbalance of the strip milled between the roll stands of the finishing mill increases or reduces strip tension. This imbalance may be caused by four main reasons, as mentioned in item 1, and in this case, the finishing mill operator is not able to keep the system stable, resulting in quality defects and impacts on production.

2.1 Main milled strip quality defects due to incorrect looper operation

According to [3] [9], there are five (5) main strip quality defects:

a- Reduction of strip width;

b- Strip rupture;

c- Strip bending;

d- Strip stretching;

e- Strip dimensional variations;

According to [3] [9], the main causes of the five milled strip quality defects due to incorrect looper operation are:

a- The low tension of the milled strip between roll stands;

This condition increases the looper angle and consequently increases the strip height between roll stands, which causes steel strip bends and further milling of bent strips. When this situation occurs, the process must be interrupted and, in some cases, the milling cylinder neck breaks.

b- High tension of the milled strip between roll stands;

This condition reduces the looper angle and consequently the strip height between roll stands, which stretches the material and causes strip rupture between roll stands, interrupting the process and in some cases requiring either the work or rest milling cylinders to be changed due to incrustations or surface defects.

2.2 Impacts on production caused by incorrect looper operation

Incorrect looper operation causes four (4) main losses in the milling process:

a- Effective use of equipment, reducing availability;

b- Product rework and deviations due to non-compliance with customer specifications;

c- Constant rework and interruptions increase processing costs;

d- Non-compliance with customer quantities and deadlines (On Time In Full - OTIF).

2.2.1 Effective use of equipment

The effective use of equipment is the percentage of time in which the equipment effectively performed its function, considering emergency downtime and excluding scheduled downtime, either for operation, maintenance, or for other reasons.

Since September of 2015, for a period of two years, the effective use has always been below the goal of 80%, in the USIMINAS Hot Strip Mill No. 2 in Cubatão, with rare exceptions over the years, as shown in Figure 4. The main reasons why the hot strip mill did not meet the desired effective use were operational emergencies, with the main cause being finishing mill scrapping, which were above 5/month, with total average scrapping of 10/month, as shown in Figure 5.

Fig.4: Effective use of Hot Strip Mill No. 2

Cubatão – USIMINAS

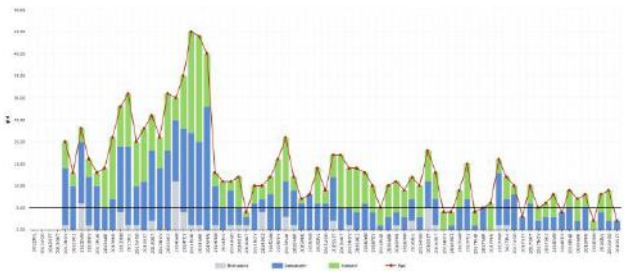

Fig.5: Occurrence of scrapping by location in Hot Strip Mill No. 2 Cubatão – USIMINAS

2.2.2 Product rework and deviations

The loss of material produced in specific pieces of equipment occurs in case of non-compliance of requirements specified by the customer and is known as rework or deviations.

2.2.2.1 Material deviations

The deviation indexes, also known as loss of material, presented the following monthly averages in respect to the total production of hot coils in Hot Strip Mill No. 2, for the following defects:

a- Incorrect width (smaller): More than 0.05% according to distribution over the years isshown in Figure 6;

b- Incorrect width (bigger): More than 0.15% according to distribution over the years is shown in Figure 7;

Incorrect width, either smaller or bigger, in respect to the nominal width defined on the customer order, occurs due to strip tension irregularities between finishing mill roll stands, as described in item 2.1 herein.

c- Thickness change: More than 0.10% according to distribution over the years is shown in Figure 8.

Thickness changes always occur after emergency downtime to remove scraps, either on the finishing mill, roughing mill, or winder. The long time required to normalize the equipment and change the work cylinders after removing scraps, mainly in the finishing mill, affects the discharge rhythm of the plate-reheating furnace and eliminates the thermal crowning of the work cylinders, requiring a new milling sequence to achieve the work cylinder thermal characteristics required, as well as plate discharge rhythm of the furnace.

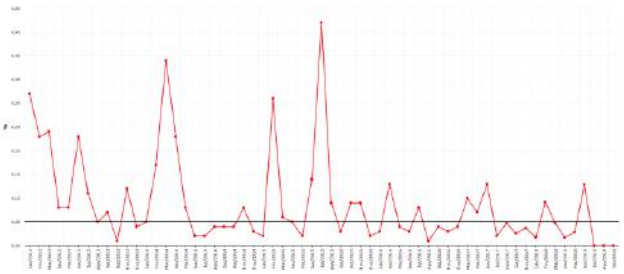

Fig.6: Incorrect width (smaller) stoppage percentage in Hot Strip Mill No. 2 – Cubatão – USIMINAS

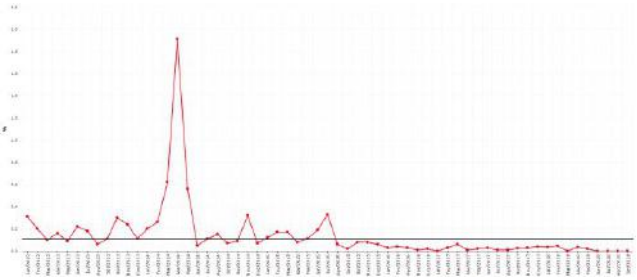

Fig.7: Incorrect width (bigger) stoppage percentage in Hot Strip Mill No. 2 – Cubatão – USIMINAS

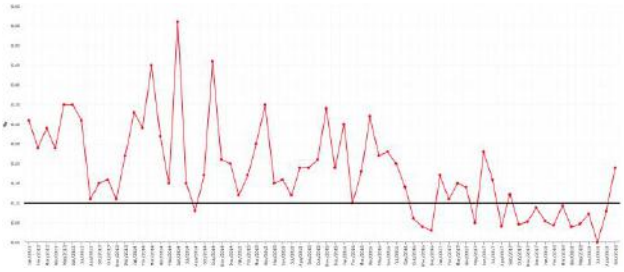

Fig.8: Thickness change stoppage percentage in Hot Strip Mill No. 2 – Cubatão – USIMINAS

2.2.2.2 Material rework

The rework indexes, also known as material rework, presented the following monthly averages in respect to the total production of hot coils in Hot Strip Mill No. 2, for the following defects:

a- Incorrect width (smaller): More than 0.20% according to distribution over the years is shown in Figure 9;

b- Incorrect width (bigger): More than 0.10% according to distribution over the years is shown in Figure 10;

The defective region of hot finishing lines must be scrapped, after the hot milling process, normally a dividing line that, in concept, besides tending to rework, divides the product within the weight range defined by the customer, using this additional process route, in cases that require rework, increasing production costs, in order to deliver the product according to the dimensions defined in the customer order.

Fig.9: Incorrect width (smaller) rework percentage in Hot Strip Mill No. 2 – Cubatão – USIMINAS

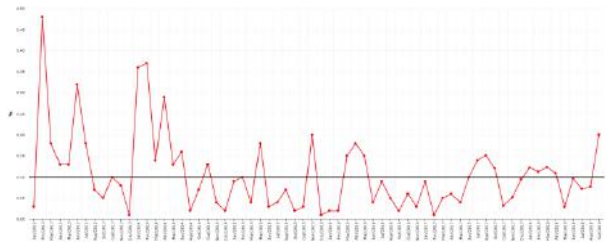

Fig.10: Incorrect width (bigger) rework percentage in Hot Strip Mill No. 2 – Cubatão – USIMINAS

2.2.3 Increased processing costs

The processing cost is defined as the total cost obtained when processing steel plates into hot coils, by means of the milling process.

The target processing cost for Hot Strip Mill No. 2 in Cubatão was U$50/t.

The results obtained over the months in 2016 and 2017 were higher than the target, as shown in Figures 11 and 12.

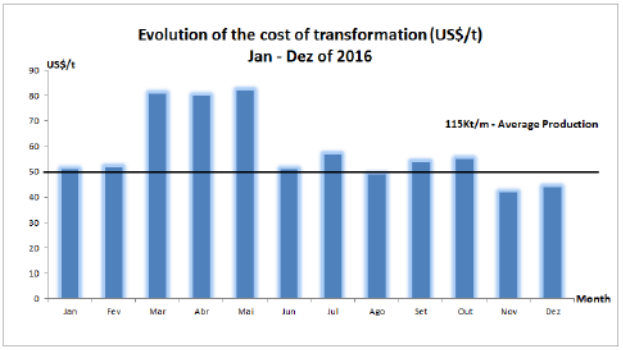

Fig.11: 2016 processing cost performance in Hot Strip Mill No. 2 – Cubatão – USIMINAS

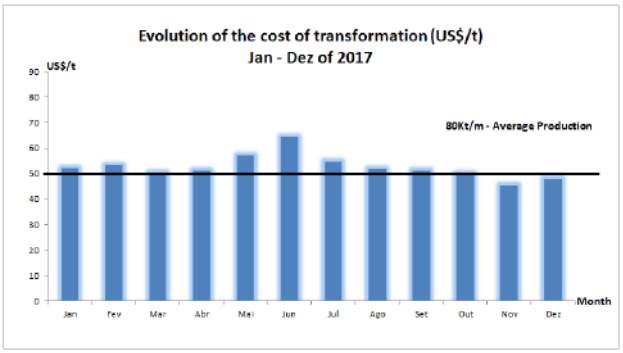

Fig.12: 2017 processing cost performance in Hot Strip Mill No. 2 -

Cubatão – USIMINAS

2.2.4 OTIF

The on time in full performance for hot coils in Hot Strip Mill No. 2 in Cubatão was lower than 60%, far from the minimum target of 80%, as shown in Figure 13.

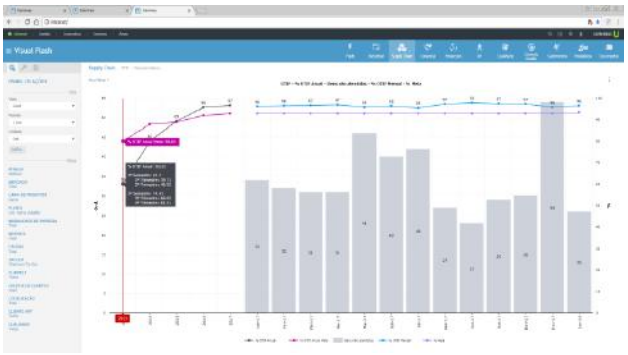

Fig.13: OTIF (On Time In Full) performance over the last 5 years in Hot Strip Mill N° 2 – Cubatão - USIMINAS

III. STEEL STRIP TENSION DYNAMIC AND STATIC MODEL USING LOOPER TORQUE AND ANGLE ACTIVE BY A SERVO VALVE

The PI and ILQ parameters are adjusted based on the steel strip tension defined and looper angle obtained in the dynamic and static model. The looper geometric relations are shown in Figure 14, and the respective nomenclatures are presented in Table 1.

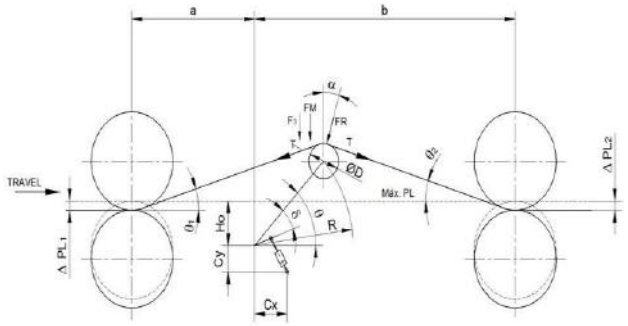

Fig.14: "Looper" and geometry between roll stands

Table 1 –" Looper" and roll stand geometry nomenclature

Symbol	Unit	Description
T	Kg	Strip tension
FS	Kg	Strip weight
FM	Kg	Bending strength
R	mm	Looper arm length
H_0	mm	Looper axial center ~ maximum distance to the pass line
H_{01}, H_{02}	mm	Looper axial center ~ expected position to pass line
$\Delta PL_1, \Delta PL_2$	mm	Difference between maximum and expected position to pass line
D	mm	Looper roll diameter
Ut	Kg/mm	Tension unit
W	mm	Strip width
t	mm	Strip thickness
ρ	Kg/mm^3	Strip density
θ	Degrees	Looper angle
θ_0	Degrees	Load cell adjustment angle
δ	Degrees	Angle between the looper arm and lever
C_X, C_Y	mm	Distance from the looper joint and cylinder joint

3.1 Strip tension calculation

The strip tension can be calculated according to the looper cylinder force. The cylinder force is detected by the pressure transducers installed in the cylinder piston and stem side cavities. The transducers calculate the tension and use it to control the looper angle. The tension calculated by the pressure load cell is used as a backup or for viewing purposes.

3.1.1 Calculation with pressureatransducer

$$T_L = T_R - J\frac{d\omega}{dt} \quad (1)$$

$$T_R = T_{LP} = I_2.F_L cos\left(\frac{\pi}{2} - \gamma - \psi\right) \quad (2)$$

Where equation 1 describes:

T_L: Looper load torque [Nm]

T_R: Torque caused by the cylinder force [Nm]

J: Looper moment of inertia + Cylinder inertia [Nm^2]

ω: Looper angular speed [rad/s]

The looper load torque is considered as the total torque by means of four torque components:

3.1.1.1 Torque due to strip tension:

$$f_3 = (\theta)A\sigma \quad (3)$$

$$f_3(\theta) = R_1\{sen(\theta + \beta) - sen(\theta - \alpha)\} \quad (4)$$

A: strip cross section (mm^2)

σ: strip unit tension (Mpa)

3.1.1.2 Torque due to strip weight:

$$f_4(\theta) \quad (5)$$

$$C = gR_1\frac{W_S}{2}\cos\,\theta \quad (6)$$

3.1.1.3 Torque due to looper weight:

$$f_5(\theta) \quad (7)$$

$$f_5(\theta) = gR_G W_L \cos\,\theta \quad (8)$$

3.1.1.4 Torque due to strip bending:

$$f_6(\theta) \quad (9)$$

$$f_6(\theta) = \frac{4E}{L^3} \mathrm{wh}^3(\mathrm{R_1 sen\theta - H_1 - R_2}) \mathrm{R_1 cos}\ \theta \quad (10)$$

Where:

$$\alpha = tan^{-1} \frac{\mathrm{R_1 sen\theta - H_1 - R_2}}{L_1 + \mathrm{R_1 cos}\ \theta} (rad) \quad (11)$$

$$\beta = tan^{-1} \frac{\mathrm{R_1 sen\theta - H_1 - R_2}}{L - L_1 + \mathrm{R_1 cos}\ \theta} (rad) \quad (12)$$

$$W_S = \rho WhL.10^{-9} (Kg) \quad (13)$$

$$T_L = f_3 A\sigma + f_4(\theta) + f_5(\theta) + f_6(\theta) \quad (14)$$

Therefore, equation 15,

$$\sigma = \frac{T_L - \left(f_4(\theta) + f_5(\theta) + f_6(\theta)\right)}{f_3(\theta) A} (MpA) \quad (15)$$

3.1.2 Calculation with a load cell

$$F_T = 2T sen \frac{\alpha + \beta}{2} \quad (16)$$

$$F_S = g.\frac{W_S}{2} \quad (17)$$

$$F_B = \frac{4EWh^3(R_1.sen\theta - H_1 + R_2}{L^3} \quad (18)$$

Where:

F_T: Strip tension [N]

F_S: Strip weight [N]

T: Total tension [N]

F_B: Torque due to strip bending:

$$\alpha = tan^{-1} \frac{H}{L_1 + L_2} \ (rad) \quad (19)$$

Where:

$$\beta = tan^{-1} \frac{H}{L - (L_1 + L_2)} (rad) \quad (20)$$

$$L_2 = R_1 cos\theta \quad (21)$$

$$H = R_1.sen\theta + R_2 - H_1 \quad (22)$$

$$W_S = \rho WhL \quad (23)$$

Where:

W: Strip width, exit from previous roll stand (mm)

h: Strip thickness, exit from previous roll stand (mm)

ρ: Steel specific weight (kg/mm^3)

δ: Load cell angle (20ºC)

The force calculated by the load cell is found using the following equation:

$$F^{\frac{L}{C}} = F_{OP}^{\frac{L}{C}} + F_{DR}^{\frac{L}{C}} = (F_T + F_S + F_B).\cos(\theta - \delta) + F_L \quad (24)$$

Where:

$$F_T = \frac{F^{LC} - F_L}{\cos(\theta - \delta)} - (F_S + F_B) \quad (25)$$

$$T = \frac{F_T}{2\ sen(\frac{\alpha+\beta}{2})} - (F_S + F_B) \quad (26)$$

$$\sigma = \frac{T}{(Wh)} \ (Mpa) \quad (27)$$

3.2 Looper model

Applying Newton's Law of movements for the looper, we have the equations and variables presented in Table 2:

$$S = \frac{(C_Y + L_C).sen(\Theta - \delta)}{\cos(\emptyset)} - L_C \quad (28)$$

$$\Theta = sen^{-1}.\left[\frac{L_3.\cos(\emptyset) - C_Y}{L_C}\right] - \delta \quad (29)$$

$$\emptyset = tan^{-1}.\left[\frac{(C_X - L_C).cos(\Theta - \delta)}{(C_Y + L_C).sen(\Theta - \delta)}\right] \quad (30)$$

$$\emptyset = \Theta_2 - \Theta_3 \quad (31)$$

$$\Theta_2 = tan^{-1}\left(\frac{C_X}{C_Y}\right) \quad (32)$$

$$\Theta_3 = cos^{-1}\left(\frac{{L_4}^2 + {L_3}^2 - {L_C}^2}{2.L_4.L_3}\right) \quad (33)$$

Table 2 – "Looper" dynamics nomenclature

Symbol	Unit	Description	Roll Stand 1 a 3	Roll Stand 4 a 5
θ	degrees	Looper angle	6,4° ~ 71,9°	6,4° ~ 71,9°
S	mm	Cylinder stroke	10 ~ 410	39,9 ~ 335,8
L_h	mm	Looper height	-44 ~ 469	-44 ~ 469
X1	mm	Cylinder shackle center on the Y axis	$X1 = Lc.sen.(\theta - \delta)$	
X2	mm	Cylinder shackle center on the X axis	$X2 = Lc.\cos.(\theta - \delta)$	
ϕ	degrees	Cylinder movement angle	$\phi = \theta_2 - \theta_3$	
L_3	mm	Cylinder shackle	$L_3 = L_0 + S$	
L_4	mm	Cylinder shackle center	1260,5	1260,5
L_0	mm	Cylinder in backward position	1111	1140,9
Cy	mm	Cylinder shackle center on the Y axis	1080	1080
Cx	mm	Cylinder shackle center on the X axis	650	650
Lc	mm	Cylinder lever length	385	280
R	mm	Arm length	612	612
δ	degrees	Arm angle	6,58°	6,58°
H_0	mm	Maximum pass line in the Y axis	205	205
D	mm	Looper roll diameter	185	185

3.2.1 Force received from the strip on the looper

For the dynamic *"looper"* load equations, the systems are according to equations 34 to 42 and Table 1, according to introduction of item 3:

$$FR = 2.T.sen.\left[\frac{(\Theta_1 + \Theta_2)}{2}\right] + FS.cos\alpha + FM.cos\alpha \quad (34)$$

$$\Theta_1 = tan^{-1}.\left[\frac{R.sen\Theta - \left(H_{O1} + \frac{D}{2}\right)}{a + R.cos\Theta}\right] \quad (35)$$

$$\Theta_2 = tan^{-1}.\left[\frac{R.sen\Theta - \left(H_{O2} + \frac{D}{2}\right)}{b + R.cos\Theta}\right] \quad (36)$$

$$H_{O1} = H_O - \Delta PL_1 \quad (37)$$

$$H_{O2} = H_O - \Delta PL_2 \quad (38)$$

$$\alpha = \frac{\Theta_2 - \Theta_1}{2} \quad (39)$$

$$T = Ut.W.t \quad (40)$$

$$FS = \frac{1}{2}.\rho.(a + b).W.t \quad (41)$$

$$FM = \frac{4.E.W.t^3\left[R.sen\Theta - \left(H_{O2} + \frac{D}{2}\right)\right]}{(a + b)^3} \quad (42)$$

3.2.2 Force received from the strip on the load cell

$$FL = \frac{FR}{2}.cos.(\Theta + \Theta_O + \alpha) \quad (43)$$

3.2.3 Force received from the "looper"

$$FR = \frac{F_{CY}.L_C.cos\Theta.cy - W_G.\cos(\Theta_G + \Theta).L}{R.\cos.(\Theta + \alpha)} + V_{OFF} \quad (44)$$

$$\Theta_{CY} = \emptyset - \Theta + \delta - acerto \pm 1°ou\ menos \quad (45)$$

3.2.4 Force received from the hydraulic cylinder

$$PH = \frac{F_{CY} + PR.AR}{AH} \quad (46)$$

3.3 Unmodeled disturbances and dynamics

There are several sources of disturbances and dynamics that affect the looper system and strip tension. The main disturbance of the strip tension circuit comes from changes in mass flow caused by the quick action of the ACY (Automatic Gauge Control) system. Another disturbance is finishing mill setup incompatibility, which creates constant disruption. In addition, forward and backward sliding, which is influenced by tension over time, is uncertain. Therefore, strip rated speed errors of 5% are frequently found. Regarding the looper angle, the unmodelled disturbances and dynamics come from vicious friction on the hydraulic cylinder, looper torque for strip bending, and so forth.

3.4 Looper hydraulic systems with cylinder controlled by a servo valve

The principle of the hydraulic looper is based on the displacement of a cylinder actuated by a four-way, three position servo valve, the principle is illustrated in Figure 5.

The hydraulic cylinder piston side is connected to a servo valve port A, and the hydraulic cylinder stem side is connected to a servo valve port B; the piston side pressure is indicated by P_{pst} and the stem side pressure is indicated by P_{rod}; the system pressure is indicated by P_{sys} and the oil return pressure is indicated by P_{tnk}; the cross-section areas of both sides of the hydraulic cylinder are indicated by $A_{pst}$and A_{rod}, and the internal and external discharge coefficient is represented by C_{in} and C_{ex} respectively; the hydraulic cylinder displacement is represented byy, and the kinematic viscosity coefficient is indicated by B; the elastic resistance coefficient is indicated by G, and the load force is indicated by F_{ld}; the

hydraulic cylinder equivalent mass and load is indicated by M, and the hydraulic oil bulk module is indicated by B_e.

There are three (3) types of oil flows in hydraulic cylinder systems controlled by servo valves, namely[12] [13] [14] [15]:

a- Hydraulic cylinder dynamic flow;

b- Servo valve specific flow;

c- Flow between the servo valve and the hydraulic cylinder.

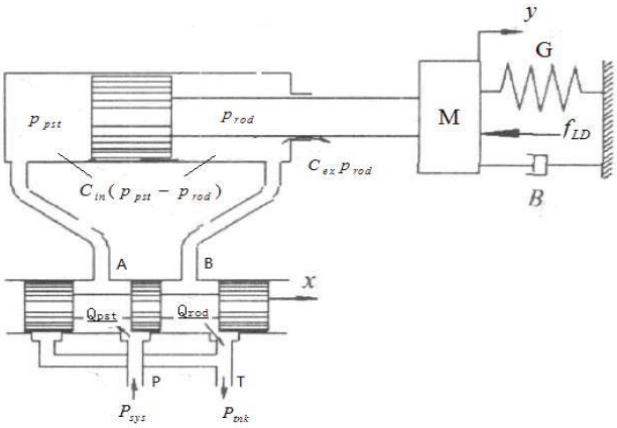

Fig.5: Hydraulic cylinder assembly activated by a servo valve

3.4.1 Analysis of the hydraulic cylinder dynamic flow

Hydraulic cylinder systems controlled by dynamic valves include pressure changes, piston movement, and flow changes caused by cavity leakage. In hydraulic cylinder systems controlled by servo valves, the flow changes for both hydraulic cylinder cavities are different.

The analysis process specifies and considers the following:

3.4.1.1 Additional flow caused by pressure changes

In the analysis process of the dynamic response of hydraulic cylinders controlled by a servo valve, oil compressibility cannot be overlooked. The relation between the addition flow for both cavities, caused by oil pressure and volume changes, is determined by means of the following equation:

$$Q_{Vpst} = \frac{V_{pst}}{B_e}.\frac{dp_{pst}}{d_t} \quad (47)$$

$$Q_{Vrod} = \frac{V_{rod}}{B_e}.\frac{dp_{rod}}{d_t} \quad (48)$$

3.4.1.2 Additional flow caused by piston displacement

The additional flow Q_{Ypst} and Q_{Yrod} for two cylinder cavities during displacement is determined by means of the following equations:

$$Q_{Ypst} = A_{pst}.\frac{d_y}{d_t} \quad (49)$$

$$Q_{Yrod} = -A_{rod}.\frac{d_y}{d_t} \quad (50)$$

3.4.1.3 Additional flow caused by leakage

The additional flows Q_{Xpst} and Q_{Xrod} for both cylinder cavities caused by leakage are directly related to their pressures. The total flow for each cavity is determined by means of the following equations:

$$Q_{Xpst} = C_{in}.(p_{pst}-p_{rod}) + C_{ex}.p_{pst} \quad (51)$$

$$Q_{Xrod} = C_{in}.(p_{rod}-p_{pst}) + C_{ex}.p_{rod} \quad (52)$$

3.4.2 Analysis of the servo valve characteristic flow

3.4.2.1 Analysis of the servo valve characteristic static flow

The characteristic flow of servo valves is described by the drop in nominal pressure Δ_{pn}, nominal flowQ_n, and the frequency response characteristic curve. When the valve pressure drop is Δ_{pn}, the relationbetween the valve actual flow and nominal flow is determined by the following equation:

$$Q(x,\Delta_{pl}) = x.Q_n.\sqrt{\frac{\Delta P_l}{\Delta P_n}} \quad (53)$$

3.4.2.2 Linearization of the servo valve characteristic static flow

The servo valve operates close to zero in respect to the opening angle, and by the linearization of the characteristic flow process, we obtain the following equation:

$$Q = K_q.x - K_c.\Delta P_L \quad (54)$$

In the equation aboveK_q, the servo valve flowK_c gain coefficient is the pressure flow coefficient. According to the servo valve flow characteristics equation, the flow gain coefficient is different and shows variation

at each change in direction and opening in degrees.

When > 0,

$$K_{q\,pst+} = Q_N.\sqrt{\frac{P_{sys} - P_{pst.0}}{\Delta P_N}} \tag{55}$$

$$K_{q\,rod} = Q_N.\sqrt{\frac{P_{rod.0} - P_{tnk}}{\Delta P_N}} \tag{56}$$

When < 0,

$$K_{q\,pst-} = Q_N.\sqrt{\frac{P_{pst.0} - P_{tnk}}{\Delta P_N}} \tag{57}$$

$$K_{q\,rod-} = Q_N.\sqrt{\frac{P_{sys} - P_{rod.0}}{\Delta P_N}} \tag{58}$$

Where, $P_{pst.0}$e $P_{rod.0}$are, respectively, the cavity static work point pressures piston side and stem side cavity. We can see that the flow gain coefficient involves four (4) parameters: $K_{q\,pst}$, $K_{q\,rod}$,$K_{q\,pst-}$and $K_{q\,rod-}$; similar to the situation of the pressure flow coefficient K_c, which make it difficult to analyze the model.

3.4.2.3 Servo valve dynamic characteristics

The actual opening X and the programmed opening of servo valves are not exactly the same, and can be described according to oscillation of two orders:

$$G_{vlv}(S) = \frac{1}{\left(\left(\frac{s}{Wv}\right)^2 + \frac{2\partial_{VS}}{W_v} + 1\right)} \tag{59}$$

Where W_v is the servo valve cut frequency,$\partial_V$is the valve core-opening coefficient.

3.4.3 Analysis of the flow between the servo valve and the hydraulic cylinder

Using the oil from each hydraulic cylinder cavity as object of research, the flow equation can be defined according to the oil continuity inside and outside the cavity.

For the piston side cavity,

$$Q_{pst}(t) = Q_{Vpst} + Q_{Ypst} + Q_{Xpst} \tag{60}$$

$$= A_{pst}.\frac{dy}{dt} + \frac{V_{pst}}{\beta_e}.\frac{dp_{pst}}{dt} + C_{in}.\left(P_{pst} - P_{rod}\right) + C_{ex}.P_{pst} \tag{61}$$

In the form of transference function,

$$P_{pst}(S) = G_{pst}(S).\left(Q_{pst} - A_{pst}.sy + C_{in}.P_{rod}\right. \tag{62}$$

Where,

$$G_{pst}(S) = \frac{1}{\left(\frac{V_{pst}}{\beta_e}S + C_{in} + C_{ex}\right)} \tag{63}$$

Likewise, for the stem side cavity,

$$Q_{rod}(t) = Q_{Vrod} + Q_{Yrod} + Q_{Xrod} \tag{64}$$

$$= -A_{rod}.\frac{dy}{dt} + \frac{V_{rod}}{\beta_e}.\frac{dp_{rod}}{dt} + C_{in}.\left(P_{rod} - P_{pst}\right) + C_{ex}.P_{rod} \tag{65}$$

In the form of transference function,

$$P_{rod}(S) = G_{rod}(S).\left(Q_{rod} - A_{rod}.sy + C_{in}.P_{pst}\right. \tag{66}$$

Where,

$$G_{rod}(S) = \frac{1}{\left(\frac{V_{rod}}{\beta_e}S + C_{in} + C_{ex}\right)} \tag{67}$$

3.4.4 Hydraulic cylinder movement equation

In the hydraulic cylinder control valve, as shown in Figure 2, according to the mechanics of Newton's Law, the hydraulic cylinder movement equation is as follows:

$$A_{pst}P_{pst} - A_{rod}P_{rod} = M\frac{d^2y}{dt^2} + B\frac{d_y}{dt^2} + Gy + f_{Ld} \tag{68}$$

In the form of transference function,

$$y(S) = G_{cyd}(S).\left(A_{pst}.P_{pst}(s) - A_{rod}.P_{rod}(s) - f_{Ld}\right) \tag{69}$$

Where,

$$G_{cyd}(S) = \frac{1}{(Ms^2 + Bs + G)} \tag{70}$$

3.5 Model of hydraulic cylinder controlled by a servo valve

3.5.1 Analysis of the static work point

The servo valve characteristic dynamic flow is always related to work point specifications, so the static work point of the hydraulic cylinder system controlled by a servo valve must be analyzed. In hydraulic cylinder systems controlled by a servo valve, as shown in Figure 5, the hydraulic cylinder must meet the following conditions to keep stationary.

3.5.1.1 Force balancing equation

When the hydraulic cylinder maintains uniform or stationary movement, the total output force of both cavities is balanced with the load.

$$A_{pst}.p_{pst} - A_{rod}.p_{rod} = f_{Ld} \tag{71}$$

The formula below is obtained when both sides of the formula above are divided byA_{rod}.

$$p_{pst} = \frac{(p_{rod} + P_{Ld})}{\varphi} \tag{72}$$

In formula,$\varphi = \frac{A_{pst}}{A_{rod}}$, $P_{Ld} = \frac{f_{Ld}}{A_{rod}}$

Obviously, the force balancing equation is a group of parallel lines for different loadsP_{Ld}.

3.5.1.2 Flow balancing equation

When the hydraulic cylinder is in uniform motion or stationary, not only the relation between the forces is maintained, but the hydraulic oil flow to the cavities also becomes proportional to the hydraulic cylinder cross-section. In other words, the hydraulic cylinder cannot move smoothly. When the cylinder stem moves in different directions, the oil path is different.

3.5.1.2.1 Hydraulic cylinder uniform forward movement

In this case, the servo valve-opening angle is$x$> 0 and the hydraulic oil flow through openings P and A of the servo valve in the hydraulic cylinder piston side cavity. The hydraulic oil flow in the stem side cavity is through openings B and T of the servo valve, returning to the hydraulic oil reservoir and expanding. According to the equations:

$$A_{pst}.v^{+} = Q_{pst} = Q_N.\sqrt{\frac{P_{sys} - p_{pst}}{\Delta P_N}} \tag{73}$$

$$A_{rod}.v^{+} = Q_{rod} = Q_N.\sqrt{\frac{P_{rod} - p_{tnk}}{\Delta P_N}} \tag{74}$$

We can, therefore, deduce that

$$p_{pst} = P_{sys} - \varphi^2(P_{rod} - P_{tnk}) \tag{75}$$

In the formula, $v^{+}$is the hydraulic cylinder movement speed; the following results are obtained considering equations (72) and (75).

$$P_{rod} = \frac{\varphi^3.P_{tnk} + \varphi.P_{sys} - P_{Ld}}{\varphi^3 + 1} \triangleq P_{rod.0^{+}} \tag{76}$$

3.5.1.2.2 Hydraulic cylinder uniform return

In this case, the servo valve-opening angle is x< 0 and the hydraulic oil flow through openings P and B of the servo valve in the hydraulic cylinder stem side cavity. The hydraulic oil flow in the piston side cavity is through opening A e T of the servo valve, returning to the hydraulic oil reservoir and retracting. According to the equations:

$$p_{pst} = P_{tnk} - \varphi^2\left(P_{sys} - P_{rod}\right) \tag{77}$$

The following results are obtained considering formulas (72) and (77).

$$P_{rod} = \frac{\varphi^3.P_{sys} + \varphi.P_{tnk} - P_{Ld}}{\varphi^3 + 1} \triangleq P_{rod.0^{-}} \tag{78}$$

From the analysis demonstrated in section 4, we know that when the hydraulic cylinder moves constantly in different directions, in general pressures $P_{rod.0+}$or $P_{rod.0-}$ on the stem sideare not the same. The force balanceequation and the flow balance equation are plotted i a plane coordinate system, as shown in Figure 6.

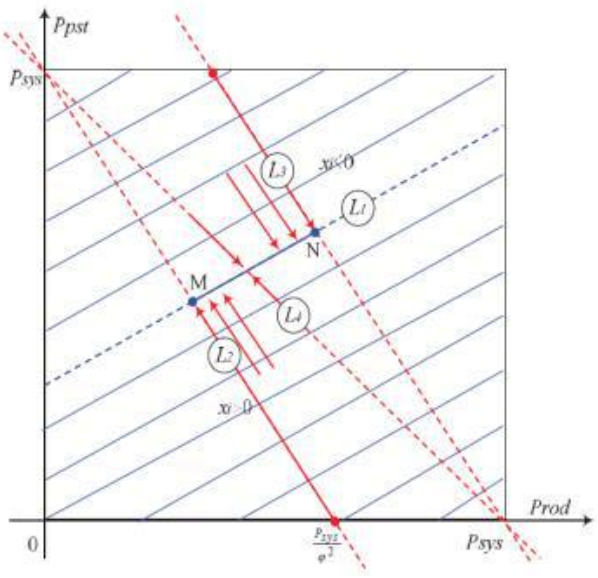

Fig.6: Static work points of hydraulic cylinders controlled by servo valves

As shown in Figure 6, the force balancing equation is represented by straight line L_1, since the cavity pressure value is positive, and is restricted to the shaded region of the graphic. Flow equations L_2, $L_3$and force balancing equation L_1have two intersection points: M and N.The analysis shows that $P_{rod\cdot 0-}$is higher than $P_{rod\cdot 0+}$, and point N is the system stable work point.

3.5.1.2.3 Symmetrical cylinder static work point

For symmetrical hydraulic cylinders with the same cross section, if the cylinder moves forwards or backward, the flow equations are the same.

$$p_{pst} = -p_{rod} + P_{sys} + P_{tnk} \tag{79}$$

The following results were obtained considering equations (72) and (79).

$$P_{rod.0} = \frac{P_{sys} + P_{tnk} - P_{Ld}}{2} \tag{80}$$

This shows that symmetrical cylinders have only one work point, which is equivalent to work points M and N of asymmetrical cylinders. According to the analysis in section 3.2, for symmetrical cylinder control valves, the flow gain coefficients for both sides of the cavity are always the same.

$$K_{q\,pst+} = K_{q\,rod+} = Q_N \cdot \sqrt{\frac{P_{sys} - P_{tnk} - P_{Ld}}{2.\Delta P_N}} \tag{81}$$

$$K_{q\,pst-} = K_{q\,rod-} = Q_N \cdot \sqrt{\frac{P_{sys} - P_{tnk} + P_{Ld}}{2.\Delta P_N}} \tag{82}$$

The equations above demonstrate that when we calculate the load flow characteristics of symmetrical hydraulic cylinders controlled by a servo valve, both cavities of the symmetrical cylinder are equivalent to one cavity, the total pressure drop of the servo valve port is the sum of the pressure drops in both servo valve openings.

3.5.2 Modeling of dynamic characteristics

In summary, the dynamic mathematical model of hydraulic cylinder systems controlled by servo valves can be obtained by means of the connection between the state variables of such systems according to the logical relationship of equations (6), (9), (11),(14), (17), as well as the demonstration in Figure 7. In Figure 7, the upper half segment reflects the piston's side cavity flow characteristics, and the lower half segment reflects the stem side cavity flow characteristics; the movement of the hydraulic cylinder connects them and some related coupling is caused by the hydraulic cylinder internal leakage.

As mentioned in section 3.2, the servo valve coefficients K_q and K_c are closely related to x (> 0 or < 0), and therefore the model shown in Figure 7 is still not a non-linear system and its dynamic and static characteristics cannot be analyzed intuitively and quantitatively, so the equivalent form of the model must be analyzed.

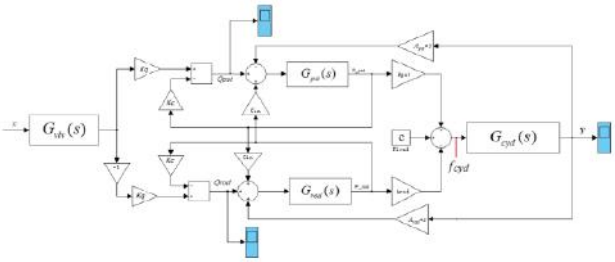

Fig.7: Dynamic model of hydraulic cylinders controlled by servo valves with a hydraulic looper

Under normal circumstances, the internal leakage coefficient C_{in} of hydraulic cylinders is very small, and both cavities create a coupling relation solely due to the movement of the hydraulic cylinder, after ignoring the leakage. The model can be simplified; the relationship between the total output force f_{cyd} of the hydraulic cylinder and the servo valve x and displacement data are as follows:

$$f_{cyd}(s) = x.\left(\frac{K_{q\,pst}.A_{pst}}{\frac{V_{pst}}{\beta_e}s + C_{ex} + K_{c\,pst}} + \frac{K_{q\,rod}.A_{rod}}{\frac{V_{rod}}{\beta_e}s + C_{ex} + K_{c\,rod}}\right) - sy.\left(\frac{A_{pst}^2}{\frac{V_{pst}}{\beta_e}s + C_{ex} + K_{c\,pst}} + \frac{A_{rod}^2}{\frac{V_{rod}}{\beta_e}s + C_{ex} + K_{c\,rod}}\right) \triangleq x.G_x(s) - sy.G_y(s) \quad (83)$$

Equations G_x(s) and G_y(s) consist of two neutral elements. For symmetrical cylinder control valves, valve coefficients $K_q$and$K_c$for both cavities are always the same, and the two neutral elements are reduced to a single element. For asymmetrical cylinder control valves, the valve coefficients for both cavities are the same. This can be approximated by the inertia element [10]. The simplified model uses a symmetrical or asymmetrical cylinder, as shown in Figure 8.

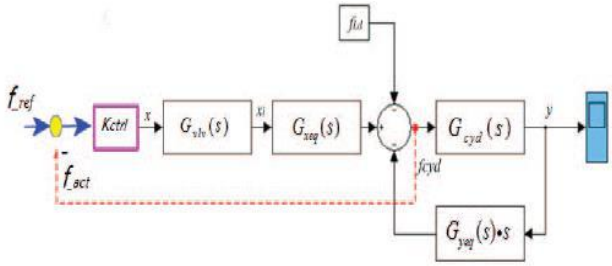

Fig.8: Simplified equivalent model of hydraulic cylinders controlled by servo valves

The closed loop control forces can be composed by introducing feedback on the hydraulic cylinder output, as shown in Figure 9, where$K_{ctrl}$is the closed loop force controller. Using the equivalent simplified model, the relationship between the excitation given x(s) and the open loop transference function $G_{xf\text{-}op}$(s) of the output force f_{cyd}(s) is as follows:

$$G_{xf-op}(s) = \frac{f_{cyd}(s)}{x(s)} = \frac{G_{vlv}(s).G_{xeq}(s)}{1 + G_{vlv}(s).G_{xeq}(s).G_{cyd}(s).G_{yeq}(s)s} \quad (84)$$

However, the closed loop transference force function $G_{xf\text{-}cl}$(s) is as follows.

$$G_{xf-cl}(s) = \frac{K_{ctrl}.G_{xf-op}(s)}{1 + K_{ctrl}.G_{xf-op}(s)} \quad (85)$$

Consequently, this is convenient to analyze system stability, dynamic characteristics, and other related indexes after using the equivalent treatment[16] [17] [18].

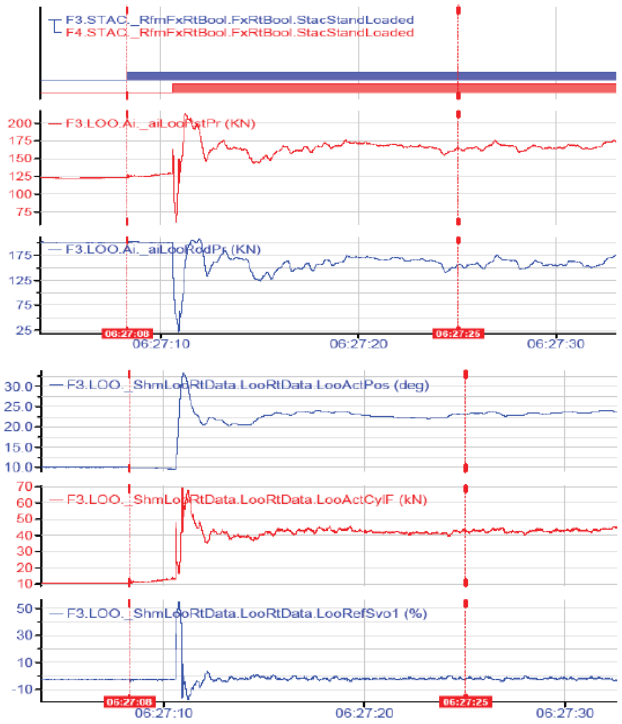

Fig.9: Practical response curve of the looper hydraulic unit closed loop control force

In hot strip finishing mill looper control systems, the closed loop force control is the main variable of the control system used in the looper hydraulic circuit.

According to looper angle changes, the output force of the hydraulic cylinder can be adjusted to maintain constant strip tension, and therefore the dynamic performance directly affects the looper response quality. Respecting the hydraulic cylinder structural data, the equivalent transference functions$G_{xeq}(s)$ e $G_{yeq}(s)$are as follows.

$$G_{xeq}(s) = \frac{12.52x10^4}{\left(\frac{s}{143.0} + 1\right)}\ (N/\%) \quad (86)$$

$$G_{yeq}(s) = \frac{2.12x10^4}{\left(\frac{s}{143.0} + 1\right)}\ (mm/\%) \quad (87)$$

The equivalent transference function mentioned above considers the flow changes in different directions of servo valves.

The simulation was conducted according to the equivalent model, as per the curves are shown in Figure 10. Before 0.3 seconds, the looper closed-loop force control element is stationary, and the pressures on both cavities are 12.4 and 20.0 Mpa, respectively. In o.3 seconds, due to the force, there is a leap of 30 kN on the force controller function, the looper hydraulic cylinder moves gradually to a new stationary state, and the pressures on both cylinder cavities change to 15.8 and 16.9 Mpa. The rise time is approximately 0.1 seconds, and the adjustment time is approximately 0.2 seconds[19] [20] [21].

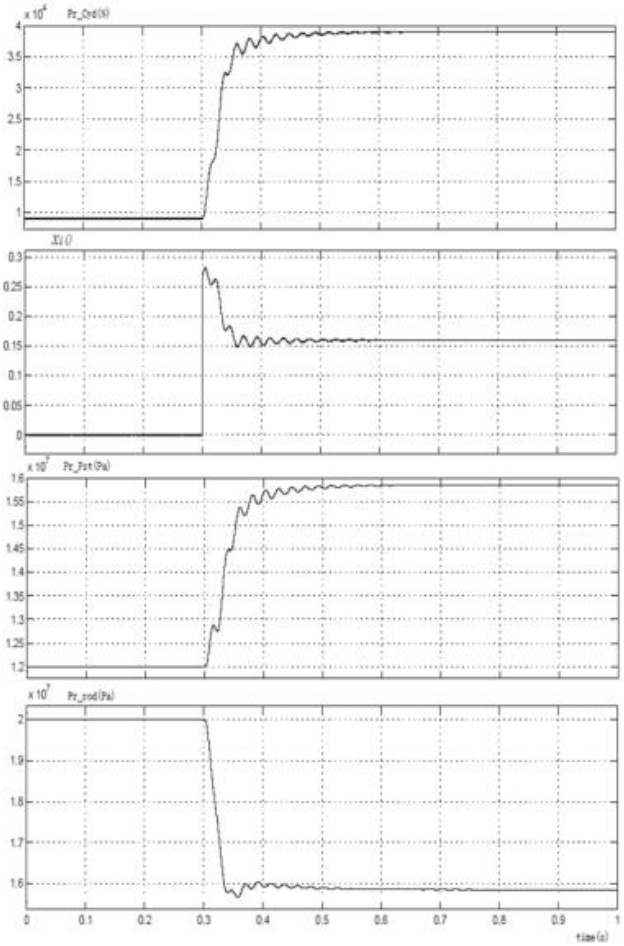

Fig.10: Response curve to closed loop force simulations in looper hydraulic units

IV. CONTROL MODES OF LOOPERS WITH HYDRAULIC CYLINDER CONTROLLED BY SERVO VALVES

4.1 ILQ control mode

ILQ control consists of strip tension and height control on the gap between the finishing mill roll stands. The strip tension and height are maintained according to the values defined by the controller, which changes the previous roll stand speed and the looper angle. The ILQ control has three (3) different control blocks that depend on the main motor and looper drive types, namely:

a- DC (Direct Current) looper electric motor and roll stand motor;

b- AC (Alternating Current) looper electric motor and roll stand motor;

c- AC (Alternating Current) looper hydraulic cylinder and roll stand motor;

Figure 11 illustrates the control diagram block forAC (Alternating Current) hydraulic cylinder and main roll stand motors, object of the present study.

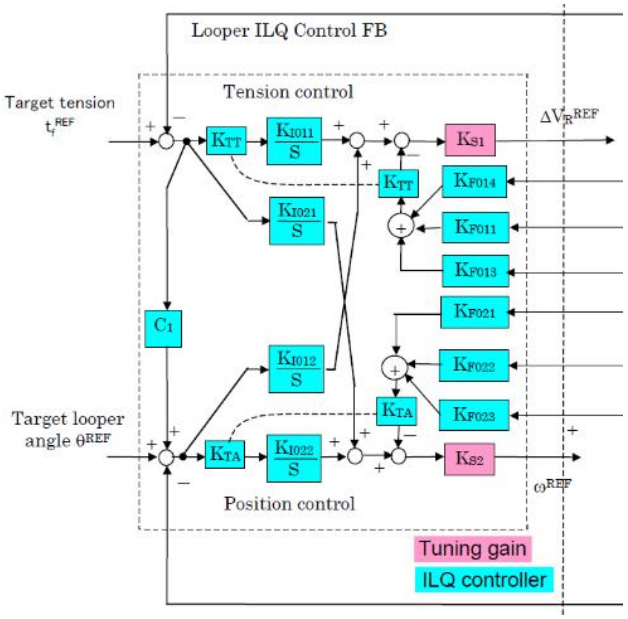

Fig.11: Control diagram block, using the position of the hydraulic cylinder in the looper and AC roll stand motor

4.2 PI control mode

The PI control is similar to the ILQ control, consisting of strip tension and height control on the gap between the finishing mill roll stands. In this mode, to maintain the defined strip tension and height values, the controller acts on the speed of the previous roll stand and looper torque.

The PI controller has the same control blocks as the ILQ controller.

Figure 12 illustrates the control diagram block for AC (Alternating Current) hydraulic cylinder and main roll stand motors, object of the present study.

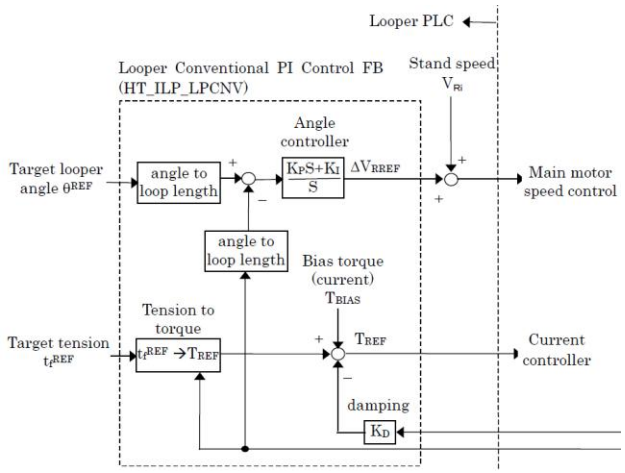

Fig.12: Control diagram block, using the torque of the hydraulic cylinder in the looper and AC roll stand motor

4.3 Predictive PI and ILQ controllers Development and parameterization of adaptive and predictive Proportional Integral (PI) e Integral Linear Quadratic (ILQ) controls.

The optimization work of both mill control modes does not require the installation of software or hardware. The control modes were optimized and improved in stages, which in the end allowed adjusting the control parameters of both control modes. The stages included:

a- Collection of strip production data and variables controlled:
  a- Product final thickness, obtained after the last roll stand of the finishing mill;
  b- Product final width, obtained after the roughing mill;
  c- Steel degree of resistance, which can be BR – Low Resistance, MR – Medium Resistance, and AR – High Resistance.

b- Looper and drive system dynamic and static modeling;

c- Analysis of the control system and operation modes;

d- Production data analysis;

e- New control mode parameterization based on stages a, b, c, and d.

f- Analysis of results and parameter adjustments.

4.3.1 Production data collection

Hot Strip Mill Nº2 in Cubatão produces nine (9) main types of steels:

a- High Strength Low Alloy Steel (HSLA);

b- High Carbon Steel;

c- Medium Carbon Steel;

e- Interstitial Free Steel – steel with low percentages of interstitial elements;

f- American Petroleum Institute Steel – steel for the oil and gas industry;

g- Dual Phase Steel;

h- Transformation-Induced Plasticity Steel (TRIP);

i- Grain Non-Oriented Steel (GNO) - steel for electrical purposes.

Each of these types of steel has specific chemical compositions, defined for level three (3) of the automation architecture of Hot Strip Mill No. 2 in Cubatão, by means of a table created from the range of each chemical element that composes these types of steel and their dimensions, either final product width or thickness. This information is essential to achieve correct mass flow control in the finishing mill, by selecting the two (2) looper control modes available for the operators, as described and presented in item 2 herein.

The main characteristics defined to collect process data are as follows:

a- Steel families;

b- Hot coil width;

c- Hot coil thickness.

4.3.1.1 Steel families

There are four (4) main components considered to define the steel families, using the quantity of each chemical component per range:

a- Basic and primary category of chemical components C, Mn, and Si;

b- Category of micro-alloy steels with chemical components Nb, Mo, V, and Ti;

c- Category of steels resistant to corrosion, with chemical component Cu;

d- Category of boron steel, with chemical component B.

Figure 13 shows the flowchart used to identify steel family categories and Tables 4 and 5 show the range of each chemical component, according to the previous definitions of the quantity of each chemical component according to the type of steel to be milled and level three of the automation architecture:

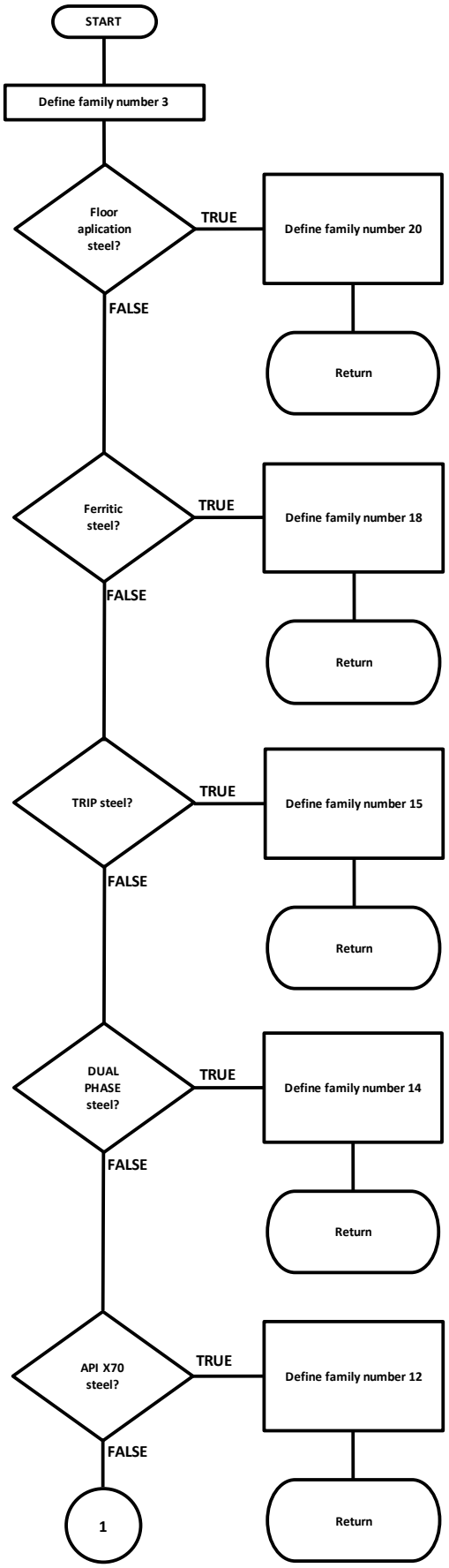

Fig.13: Steel family flow chart

Table 4 - Steel families and chemical composition ranges

Steel Family	Steel Description	Carbon Range	Alloy Range
1	Ultra Low Carbon	C ≤ 0,01	-
2	Ultra Low Carbon and IF	C ≤ 0,01	$(Nb_1\ ou\ Ti_1\ ou\ Mo_1\ ou\ V_1\ ou\ B_1)$
3	Low Carbon	0,01 < C ≤ 0,25	-
4	Low Carbon and Corrosion Resistant	0,01 < C ≤ 0,25	Cu_1
5	Low Carbon and Micro Alloy	0,01 < C ≤ 0,25	$(Nb_2\ ou\ Ti_2\ ou\ Mo_2\ ou\ V_2)$
6	Low Carbon and Boron Inclusion	0,01 < C ≤ 0,25	B_2
7	Medium Carbon	0,01 < C ≤ 0,55	-
8	Medium Carbon and Micro Alloy	0,01 < C ≤ 0,55	$(Nb_3\ ou\ Ti_3\ ou\ Mo_3\ ou\ V_3)$
9	Medium Carbon and Boron Inclusion	0,01 < C ≤ 0,55	B_3
10	High Carbon	0,55 ≤ C	-
11	Manganese	-	Mn_1
12	X56 and X70 Tubes	-	Value defined by the client on the sales order
13	Tubes above X80	-	Value defined by the client on the sales order
14	Dual Phase	-	Value defined by the client on the sales order
15	TRIP	-	Value defined by the client on the sales order
16	NGO	-	Si_1
17	RCO	-	Si_2
18	Ferritic	-	Value defined by the client on the sales order
19	X42 and X46 Tubes	-	Value defined by the client on the sales order
20	Floor Plates	-	-

Table 5 - Alloy component patterns

Chemical Element	Symbol	Threshold Value
C	C_1	0,01
	C_2	0,25
	C_3	0,55
Si	Si_1	0,50
	Si_2	0,95
B	B_1	0,05
	B_2	0,05
	B_3	0,05
Cu	Cu_1	0,15
Nb	Nb_1	0,008
	Nb_2	0,008
	Nb_3	0,008
Ti	Ti_1	0,01
	Ti_2	0,01
	Ti_3	0,01

Chemical Element	Symbol	Threshold Value
Mo	Mo_1	0,021
	Mo_2	0,021
	Mo_3	0,021
V	V_1	0,018
	V_2	0,018
	V_3	0,018
Mn	Mn_1	1,29

4.3.1.2 Hot coil dimensions

Hot Strip Mill Nº2 in Cubatão produces hot coils with the following final product width and thickness dimensions:

a- Width: 750 to 2050 mm

b- Thickness: 1.5 to 20 mm

These dimensions were divided into ranges: there are eight (8) width ranges and twenty (20) thickness ranges, all according to the dimensions of the final product. These dimensions and ranges are included in each of the twenty (20) steel families defined in item 4.3.1.1.

Table 6 shows the looper unit tensions for family 8 steels: medium micro-alloy carbon steel with 700 to 900 mm in width.

Table 7 shows the looper unit tensions for family 8 steels: medium micro-alloy carbon steel with 1350 to 1500 mm in width.

Table 6 – Looper unit tensions for family 8 steels with 700 to 900 mm width, per thickness range

Width Index (mm)		Thickness Index (mm)		Looper Unit Tension for each roll stand gap (Mpa)				
				F1-F2	F2-F3	F3-F4	F4-F5	F5-F6
1	700 <= w < 900	1	1.2 <= h < 1.3	5,3	8,5	10,9	18,2	23,3
		2	1.3 <= h < 1.5	5,2	8,2	10,6	17,4	22,2
		3	1.5 <= h < 1.7	8,0	11,0	14,0	16,0	20,5
		4	1.7 <= h < 1.9	8,0	11,0	14,0	16,0	19,0
		5	1.9 <= h < 2.2	8,0	11,0	14,0	16,0	19,0
		6	2.2 <= h < 2.5	7,0	9,5	11,5	13,5	16,0
		7	2.5 <= h < 2.9	6,0	8,5	10,5	12,5	15,0
		8	2.9 <= h < 3.4	6,0	8,5	10,5	12,5	15,0
		9	3.4 <= h < 4.0	6,0	8,5	10,5	12,5	15,0
		10	4.0 <= h < 5.0	5,0	7,5	9,5	11,5	14,0
		11	5.0 <= h < 6.5	4,1	5,5	6,8	10,0	12,0
		12	6.5 <= h < 8.0	3,9	5,2	6,4	9,2	10,8
		13	8.0 <= h < 9.5	3,8	4,9	6,0	8,5	10,0
		14	9.5 <= h < 11.0	3,7	4,7	5,7	8,0	9,3
		15	11.0 <= h < 13.0	3,6	4,5	5,5	7,5	8,7
		16	13.0 <= h < 15.0	3,5	4,3	5,2	7,1	8,1
		17	15.0 <= h < 17.0	3,4	4,1	5,0	6,7	7,7
		18	17.0 <= h < 19.0	3,3	4,0	4,8	6,4	7,3
		19	19.0 <= h < 22.0	3,3	3,9	4,6	6,1	6,9
		20	22.0 <= h	3,2	3,7	4,5	5,8	6,6

Table 7 – Looper unit tensions for family 8 steels with 1350 to 1500 mm width, per thickness range

Width Index (mm)		Thickness Index (mm)		Looper Unit Tension for each roll stand gap (Mpa)				
				F1-F2	F2-F3	F3-F4	F4-F5	F5-F6
4	1350 <= w < 1500	1	1.2 <= h < 1.3	5,4	8,7	11,5	18,4	23,5
		2	1.3 <= h < 1.5	5,3	8,4	11,1	17,6	22,3
		3	1.5 <= h < 1.7	10,0	13,0	16,0	18,0	22,5
		4	1.7 <= h < 1.9	10,0	13,0	16,0	18,0	21,0
		5	1.9 <= h < 2.2	10,0	13,0	16,0	18,0	21,0
		6	2.2 <= h < 2.5	9,6	12,1	14,5	16,5	19,5
		7	2.5 <= h < 2.9	9,6	12,1	14,5	16,5	19,5
		8	2.9 <= h < 3.4	9,6	12,1	14,5	16,5	19,5
		9	3.4 <= h < 4.0	9,6	12,1	14,5	16,5	19,5
		10	4.0 <= h < 5.0	8,6	11,1	13,5	15,5	18,5
		11	5.0 <= h < 6.5	6,2	7,7	10,2	13,2	15,1
		12	6.5 <= h < 8.0	4,0	5,3	6,7	9,3	10,9
		13	8.0 <= h < 9.5	3,9	5,0	6,3	8,6	10,1
		14	9.5 <= h < 11.0	3,8	4,8	6,0	8,1	9,4
		15	11.0 <= h < 13.0	3,7	4,6	5,7	7,6	8,8
		16	13.0 <= h < 15.0	3,6	4,4	5,4	7,2	8,2
		17	15.0 <= h < 17.0	3,5	4,3	5,2	6,8	7,7
		18	17.0 <= h < 19.0	3,4	4,1	5,0	6,5	7,4
		19	19.0 <= h < 22.0	3,3	4,0	4,8	6,2	6,9
		20	22.0 <= h	3,3	3,8	4,7	5,9	6,6

4.3.1.3 Looper unit tension

As described in item 1, there is a looper installed between each finishing mill roll stand. Due to the dimensions (width, and thickness), within each of the 230 steel families, there are unit tensions for each looper. These tensions are references used by the controllers to maintain the correct mass flow between each finishing mill roll stand, according to item 4. Figure 14 shows the unit tensions applied before implementing the study herein, and Figure 15 shows the unit tensions applied after the implementation:

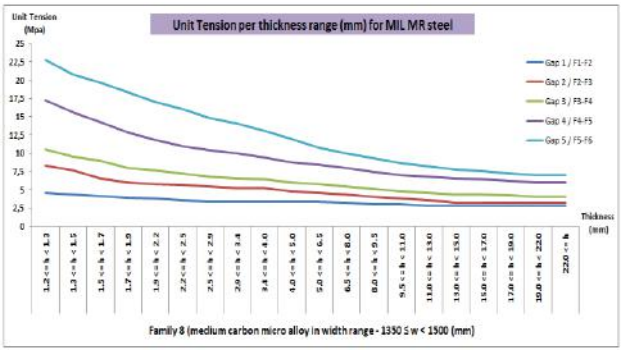

Fig.14: Unit tensions before implementation

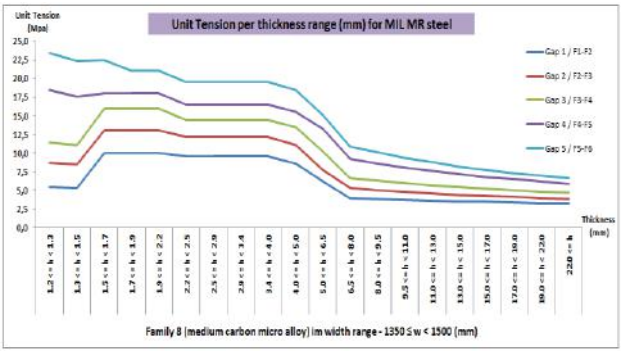

Fig.15: Unit tensions after implementation

4.3.2 Looper dynamic model and analysis of operational modes

These stages are described and presented in item 2 herein.

4.3.3 Production data analysis

After implementing the new unit tensions, using the reference variables defined in the previous items, to validate the operation mode appropriate for each of the steel families and dimensions. The appropriate looper control mode to be used by the production operators in the finishing mill is defined by two groups:

a- For materials with a thickness of more than 6 mm and width of more than 1500 mm, in the Table 8 defines the operation modes for each looper in the finishing mill:

Table 8 – Looper operation modes defined for item a

Gap between roll stands	Operation Mode
1~2	ILQ
2~3	ILQ
3~4	ILQ
4~5	PI
5~6	PI

b- For materials with a thickness of less than 6 mm and width of less than 1500 mm, in the Table 9 defines the operation modes for each looper in the finishing mill:

Table 9 – Looper operation modes defined for item b

Gap between roll stands	Operation Mode
1~2	ILQ
2~3	ILQ
3~4	ILQ
4~5	ILQ
5~6	ILQ

4.3.4 New parameterization of control modes

The models were followed -up over a period, with adjustments and adaptations to better represent looper control during the milling process.

Historical data was followed-up to allow interventions in order to avoid incidents during the milling process.

In the ILQ model, the interventions were made on the two main control variables, with changes in the loop gains:

a- Tension control: Gain adjustment of variables K_{TT} and K_{S1}, for tensions between roll stands, reducing or increasing the speed of the previous stand to ensure the correct mass flow, as shown in Chapter 5, Item

5.1 and Figure 11.

b- Position control: Gain adjustment of variables K_{TA} and K_{S2}, for looper angles, reducing or increasing the height to ensure

the correct mass flow, as shown in Chapter 5, Item5.1 and Figure 11.

In the PI model, the interventions were made on the two main control variables, with changes in the loop gains:

a- Tension control: Gain adjustment of the variable K_{PS}, for tensions between roll stands, reducing or increasing the speed of the previous stand to ensure the correct mass flow, as shown in Chapter 5, Item 5.2 and Figure 12.

b- Torque control: Gain adjustment of the variable K_D,for looper torque, reducing or increasing the height to ensure the correct mass flow, as shown in Chapter 5, Item 5.2 and Figure 12.

4.3.5 Analysis of results

After the changes implemented in models ILQ and PI, we achieved improvements in the following process indicators of Hot Strip Mill Nº2:

a- Effective use: More than 82% for six consecutive months, unprecedented performance in the process, as shown in Figure 23;

b- Finishing mill scrapping: InSeptember 2017 and February 2018, with zero scrapping results, as shown in Figure 24;

c- Drop or deviations: Less than 0.4% for six consecutive months, unprecedented performance, as shown in Figure 25;

d- Rework: Less than 3% for five consecutive months, as shown in Figure 26;

e- Processing costs: Average lower than U$50/t in 2017; lowest value in November with U$46/t, as shown in Figure 27;

f- OTIF: Average over 2017 of 96.57%, unprecedented performance, as shown in Figure 28.

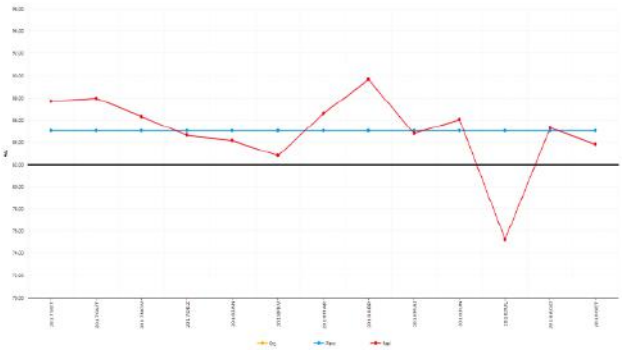

Fig.23: 2017 effective use performance in Hot Strip Mill Nº2 – Cubatão – USIMINAS

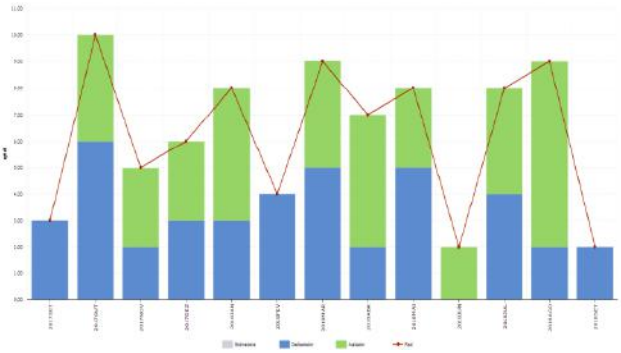

Fig.24: 2017 scrapping performance in Hot Strip Mill Nº2 – Cubatão – USIMINAS

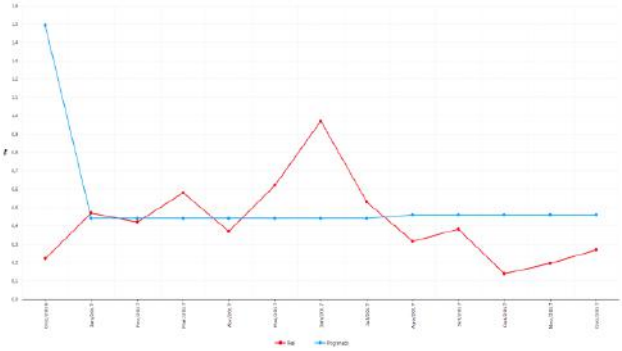

Fig.25: 2017 loss or deviation performance in Hot Strip Mill Nº2 – Cubatão – USIMINAS

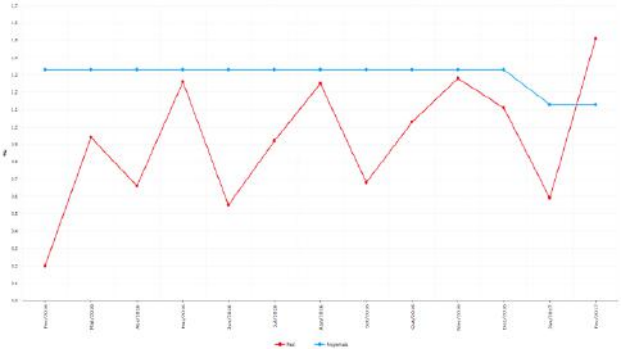

Fig.26: 2017 rework performance in Hot Strip Mill Nº2 – Cubatão – USIMINAS

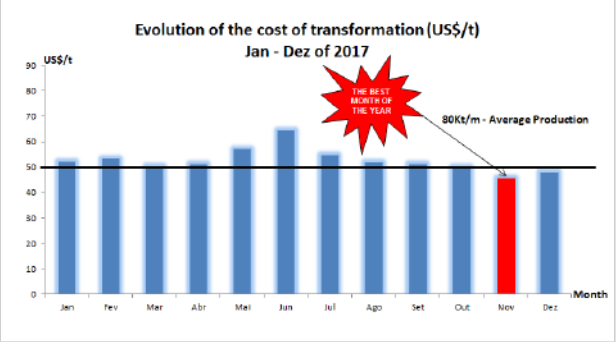

Fig.27: November 2017 processing cost performance in Hot Strip Mill Nº2 – Cubatão – USIMINAS

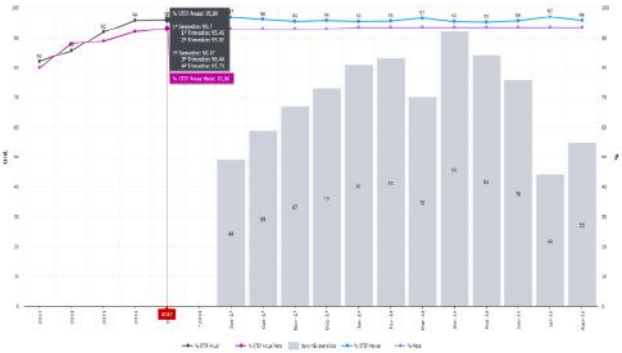

Fig.28: 2017 OTIF (On Time In Full) performance in Hot Strip Mill Nº2 – Cubatão - USIMINAS

V. CONCLUSIONS

Currently, as described in the introduction herein, the production of hot strip coils in Hot Strip Mill No. 2 of USIMINAS– Usina Siderúrgica de Minas, in the city of Cubatão in Brazil, employs two control systems: PI and ILQ.

These systems operate satisfactorily, as described in item 2, but there are quality issues and impacts on production.

The main purpose of the present research work show herein is to create a procedure to allow production operators to take appropriate decisions regarding the type of controller to be used and the controller parameters to be employed.

This regulatory procedure shall significantly eliminate the quality issues described in item 2 herein; therefore, we developed the looper dynamic and static models to obtain the looper control modes described in item 4 above. The new regulatory procedure was implemented in continuous operation, and the production obtained was analyzed as presented in item 4.3.5 herein; six significant production and quality improvements were obtained.

Therefore, we can conclude that the development and application of the new regulatory procedure contributed significantly to improve global production.

To continue the survey, we suggest that the relationship between the PI or ILQ control modes and respective parameter adjustments shall be automated employing Artificial Intelligence techniques, in order to incorporate industry 4.0 parameters in the productive sector.

REFERENCES

[1] I. S. Choi, J. A. Rossiter, and P. J. Fleming, “Looper and tension control in hot rolling mills: A survey,” Journal of Process Control, vol. 17, pp. 509–521, 2007.

[2] H. Asada, A. Kitamura, S. Nishino, and M. Konishi, “Adaptive and Robust Control Method with Estimation of Rolling Characteristics for Looper Angle Control at Hot Strip Mill,” ISIJ International, vol. 43, no.3, pp. 358–365, 2003.

[3] Y. Seki, K. Sekiguchi, Y. Anbe, K. Fukushima,

[4] Y. Tsuji, and S. Ueno, “Optimal Multivariable Looper Control for Hot Strip Finishing Mill,”

[5] IEEE Transactions on Industry Applications, vol. 27, no. 1, pp. 124–130, January/February 1991.

[6] H. Imanari, Y. Morimatsu, K. Sekiguchi, H. Ezure, R. Matuoka, A. Tokuda and H. Otobe, “Looper H-Infinity Control for Hot-Strip Mills,” IEEE Transactions on Industry Applications, vol. 33, no. 3, pp. 790–796,1997.

[7] G. Hearns, and M. J. Grimble, “Robust Multivariable Control for Hot Strip Mills,” ISIJ International, vol. 40, no. 10, pp. 995-1002, 2000.

[8] F. A. Cuzzola, “Multi-Objective Approach for the Control of Hot-Strip Mills,” Journal of Dynamic Systems, Measurement, and Control, vol. 128, no. 2, pp. 856–868, December 2006.

[9] B. Q. Li, K. J. Zhang, J. Fu, and Y. K. Sun, “Diagonal Recurrent Neural Network Decoupling Control on The Looper's Height and Tension System,” in Proceedings of the 6th World Congress on Control and Automation, Dalian, China, June 21- 23, 2006, pp. 2787–2791.

[10] R. Furlan, F. A. Cuzzola, and T. P. Parisini, “Friction compensation in the interstand looper of hot strip mills: A sliding-mode control approach,” Control Engineering Practice, vol. 16, pp. 214-225, 2008.

[11] T. Hesketh, Y. A. Jiang, D. J. Clements, D. H. Butler, and R. Laan, “Controller Design for Hot Strip Finishing Mills,” IEEE Transactions on Control Systems Technology, vol. 6, no. 2, pp. 208– 219, 1998.

[12] I. C. Hwang, and C. J. Park, “Nonlinear Looper-Tension Control for Hot Strip Finishing Mill Using Feedback Linearization,” in Proceedings of the 17th World Congress of the International Federation of Automatic Control, Seoul, Korea, July 6-11, 2008, pp. 1659–1660.

[13] H. K. Khalil, Nonlinear Systems. Prentice Hall Inc., 2007, ch. 14.1.

[14] X.N. Li, Y.Y. Han, "The Simulation of Valve- controlled Hydraulic base on SIMULINK," Equipment Manufacturing Technology, 2010, (2):30- 2. (in Chinese)
[15] K. Dasgupta, H. Murrenhoff, "Modelling and dynamics of a servo-valve controlled hydraulic motor by bondgraph," Mechanism and Machine Theory, 2011, 46(7): 1016-1035.
[16] B. Eryilmaz, B.H. Wilson, "Unified modeling and analysis of a proportional valve," Journal of the Franklin Institute, 2006, 343(1): 48-68.
[17] Y. Shen, X.D. Gao, J. Wang, "Model and Analysis of Electro-hydraulic Proportional Displacement Control System Based on Asymmetric Hydraulic Cylinder Controlled Symmetrical Valve," Journal of Shaanxi University of Science & Technology, 2007, 25(4): 105-109. (in Chinese)
[18] S. Xiao, B.M. Qiang, "The Model and Simulation of Electro-hydraulic Proportional Position-control System Based on Asymmetrical Hydraulic Cylinder Controlled by Symmetrical Four-way Valve," Machine Tool & Hydraulics, 2009, 37(6): 95-98. (in Chinese)
[19] G.Y. Jiang, Y.Q. Wang, X.C.Yan, "Mathematics Modeling and Simulation Analysis of Dynamic Characteristics for Hydraulic Cylinder Controlled by Servo-valve," Journal of Sichuan University (Engineering Science Edition), 2008, 40(5): 195-198. (in Chinese)
[20] B.M. Qiang, B.J. Liu, "A Study of modeling of Valve Controlled Asymmetry Hydraulic Cylinder," Equipment Manufacturing Technology, 2011, (3): 9-12. (in Chinese)
[21] C.L. Wang, F. Ding, Q.P. Li, Q.S. Yang, "Research on Dynamic Characteristics of symmetric Cylinder Controlled by Symmetric Fourway Valve," China Mechanical Engineering, 2004, 15(6): 471-475. (in Chinese)
[22] Y.M. Xu, Analysis,and Design of Electrohydraulic Proportional Control System, China Machine Press, 2005. (in Chinese)
[23] Y.S. Li, Automatic Control Principle, 3rd ed., National Defense Industry Press, 2005. (in Chinese)